FULL-PARTICLE SIMULATIONS ON ELECTROSTATIC PLASMA ENVIRONMENT NEAR LUNAR VERTICAL HOLES Y. Miyake[1] and M. N. Nishino[2], [1]Education Center on Computational Science and Engineering, Kobe University, Japan. (y-miyake@eagle.kobe-u.ac.jp) [2]Institute for Space-Earth Environmental Research, Nagoya University, Japan.

Introduction: The Kaguya satellite and the Lunar Reconnaissance Orbiter have observed a number of vertical holes on the terrestrial Moon [1,2], which have spatial scales of tens of meters and are possible lava tube skylights. The hole structure has recently received particular attention, because the structure gives an important clue to the complex volcanic history of the Moon. The holes also have high potential as locations for constructing future lunar bases, because of fewer extra-lunar rays/particles and micrometeorites reaching the hole bottoms. In this sense, these holes are not only interesting in selenology, but are also significant from the viewpoint of electrostatic environments. The subject can also be an interesting resource of research in planetary science, because hole structures have been found in other solar system bodies such as the Mars.

The lunar dayside electrostatic environment is governed by electrodynamic interactions among the solar wind plasma, photoelectrons, and the charged lunar surface, providing topologically complex boundaries to the plasma. We perform the three-dimensional, massively-parallelized, particle-in-cell simulations to reproduce the near-hole plasma environment on the Moon [3].

Simulation Method and Model: The simulations were performed using our original plasma particle code called EMSES, originally developed for spacecraft-plasma interaction study [4]. EMSES is based on the standard electromagnetic PIC method [5]. The plasma is modeled as an aggregation of a huge number of charged macro-particles, whereas the electromagnetic field components are defined discretely on the computational grid points. In the current study, we ran the code in the electrostatic mode, in which Poisson's equation for an electrostatic field and Newton's equations of motion for plasma macro-particles are solved simultaneously as basic equations.

The topographical structure of the lunar vertical hole is described as internal boundaries in the simulations. In the Cartesian coordinate system used in EMSES, we take the z axis to be the vertical direction and assume an xy (z=0) plane as the lunar plain ground. In the center of the ground, we model a vertical hole with a diameter of 50 m and a depth of 45 m. A plane 60 m under the ground (i.e., 15 m under the bottom surface of the hole) is taken as the lower simulation boundary. The three-dimensional simulation domain consists of 400×400×2000 grid points. We solve about 25 billion plasma macro-particles throughout the simulations. The grid width of 0.5 m is comparable to the plasma Debye length near the surface. We employ the Dirichlet boundary condition for the lower and upper simulation boundaries and a periodic condition for the lateral simulation boundaries. The lunar surface is regarded as an insulator; i.e., the charge of impinging plasma particles is accumulated at their incident positions on the surface. We took into account the solar wind plasma downflow and the photoelectron emission from the sunlit part of the lunar surface. The nominal parameters are used for the density, temperature, and bulk flow speed of these plasma species.

Lunar Surface Charging: Figure 1 displays the potential distribution on the lunar surface for solar zenith angle 30°. The potential is referenced to the value at 1 km above the lunar ground, which can be regarded as the space potential in the solar wind. The sunlit part of the ground and hole surface is charged positively, ranging from a few to 20 V, which is due to solar wind proton impact as well as photoelectron release from the surface. At the shadowed region, on the other hand, these two factors hardly contribute to the charging. Instead, some high energy portion of the thermalized electrons can contribute to the negative charging (a few tens of V) of the surface. At the interface between the sunlit and shaded region, the locally high potential (20 V at maximum) stands out from the rest of the sunlit part. This overshooting potential greatly amplifies the electric field from the sunlit to shadowed regions. Although not displayed graphically, local maximum fields of a few tens of V/m are observed in the simulation at the rim and

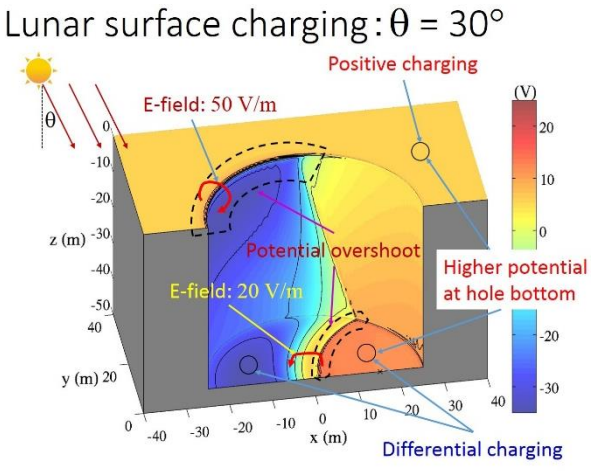

Fig.1 Electric potential mapping on the lunar surface

bottom of the hole, respectively, which are much greater than the field predicted at the edge of a typical impact crater [6].

The potential of several V observed at the sunlit lunar ground is consistent with previous predictions [6]. A remarkable finding is that the sunlit face of the hole bottom has a higher potential than that of the lunar ground. Note that the photoelectron yield from the sunlit hole bottom and the lunar ground is identical in the present situation. This suggests that some other current components are responsible for the potential difference. We next examine the plasma behavior near the lunar surface and show that there is a significant difference between the inside and outside of the hole.

Plasma Dynamics Around the Hole: Figure 2 shows the plasma and potential distribution for the solar zenith angle 30° in an xz plane that cuts the center of the hole, plotted with plasma flow vectors. Because solar wind protons have much greater flow energy (about 1 keV) than electrostatic potential energy inside the hole, they show nearly ballistic motion within the hole, which creates a clear boundary separating the space into domains with and without proton flux. Meanwhile, solar wind electrons are subject to the local potential structure and its associated electric field. In Figure 2b, the solar wind electron density shows a significant decrease inside the hole. This is due primarily to the shaded domain with large negative potential. Another reason is the absorption of electrons at the sunlit part of the vertical wall. As shown in Figure 2d, the vertical wall is charged positively, and thus a substantial portion of the electrons are trapped by the potential. Consequently, a fraction of the solar wind electrons can approach the hole bottom, which leads to the density reduction inside the hole. These factors clearly reduce the solar wind electron current flowing into the hole bottom. This is the main factor producing the higher potential at the hole bottom than that outside the hole.

Another interesting feature is a downward flow of photoelectrons seen deep inside the hole in Figure 2c. In the mid-depth region of the hole, the electric field consists of an intense horizontal component pointing in the -x direction and a weak vertical component of the upward direction. Among them, the upward electric field component produces the downward bulk flow of photoelectrons. As a marked feature, the downward photoelectron flow dominates over the photoelectron (upward) outflow from the hole bottom. This is very different from the hole exterior, which shows an upward photoelectron flow.

Conclusions: As a striking finding, the self-consistent modeling also predicts a potential difference between the sunlit surfaces inside and outside the hole.

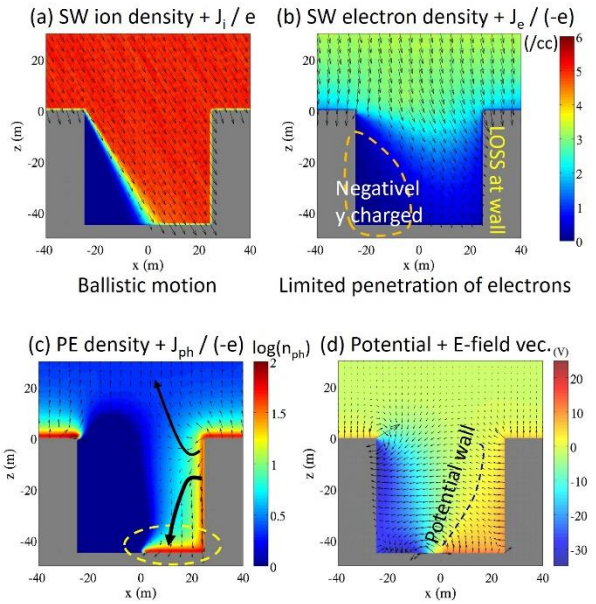

Fig.2 Two-dimensional (xz) slices of (a) electric potential with electric field vectors and (b) solar wind proton, (c) solar wind electron, and (d) photoelectron densities with their flow vectors near the vertical hole.

This reflects the change of the plasma dynamics inside the hole, particularly the solar wind and photoelectron flow patterns due to the hole-interior electric field and the presence of the vertical wall as an electron absorbing boundary. The resultant current balance condition established at the hole bottom is found to be totally different from that outside the hole, and the altered condition produces a higher potential at the hole bottom as long as the surface is in a sunlit condition. The results exhibit the uniqueness of the vertical hole environment among the various topographies on the Moon. The present work should be followed by an assessment of the dust environment around lunar vertical holes, which would provide important information for future lunar landing missions.

References: [1] Haruyama J. et al. (2009) *GRL, 36,* L21206. [2] Robinson M. S. et al. (2012) *Planet. Space Sci., 69,* 18-27. [3] Miyake Y. and Nishino M. N. (2015) *Icarus, 260,* 301-307. [4] Miyake Y. and Usui H. (2009) *Phys. Plasmas, 16,* 062904. [5] Birdsall C. K. and Langdon A. B. (1985), *Plasma Physics via Computer Simulation*. [6] Poppe A. et al. (2012) *Icarus, 221,* 135-146.